View metadata, citation and similar papers at core.ac.uk

brought to you by CORE

provided by University of Strathclyde Institutional Repository

Controlled merging and annihilation of localised dissipative structures in an AC-driven damped nonlinear Schrödinger system

This content has been downloaded from IOPscience. Please scroll down to see the full text.

2016 New J. Phys. 18 033034

(http://iopscience.iop.org/1367-2630/18/3/033034)

View the table of contents for this issue, or go to the journal homepage for more

Download details:

IP Address: 130.159.82.179
This content was downloaded on 01/04/2016 at 15:16

Please note that terms and conditions apply.

New Journal of Physics
The open access journal at the forefront of physics

Deutsche Physikalische Gesellschaft DPG
IOP Institute of Physics

Published in partnership with: Deutsche Physikalische Gesellschaft and the Institute of Physics

OPEN ACCESS

RECEIVED
3 November 2015

REVISED
9 February 2016

ACCEPTED FOR PUBLICATION
1 March 2016

PUBLISHED
24 March 2016

Original content from this work may be used under the terms of the Creative Commons Attribution 3.0 licence.

Any further distribution of this work must maintain attribution to the author(s) and the title of the work, journal citation and DOI.

PAPER

Controlled merging and annihilation of localised dissipative structures in an AC-driven damped nonlinear Schrödinger system

Jae K Jang[1,3], Miro Erkintalo[1], Kathy Luo[1], Gian-Luca Oppo[2], Stéphane Coen[1] and Stuart G Murdoch[1]

[1] Dodd-Walls Centre and Department of Physics, The University of Auckland, Private Bag 92019, Auckland 1142, New Zealand
[2] SUPA and Department of Physics, University of Strathclyde, Glasgow G4 0NG, UK
[3] Current address: Department of Applied Physics and Applied Mathematics, Columbia University, New York, NY 10027, USA

E-mail: s.coen@auckland.ac.nz

Keywords: nonlinear resonator, localised dissipative structure, soliton interaction, dissipative systems

Abstract

We report studies of controlled interactions of localised dissipative structures in a system described by the AC-driven damped nonlinear Schrödinger equation (equivalent to the Lugiato–Lefever model). Extensive numerical simulations reveal a variety of interaction scenarios that are governed by the properties of the system driver, notably its gradients. In our experiments, performed with a nonlinear optical fibre (Kerr) resonator, the phase profile of the driver is used to induce interactions of the dissipative structures on demand. We observe both merging and annihilation of localised structures, i.e. interactions governed by the dissipative, out-of-equilibrium nature of the system. These interactions fundamentally differ from those typically found for conventional conservative solitons.

1. Introduction

Localised structures coexisting with a homogeneous background are ubiquitous phenomena in extended dissipative systems driven far from equilibrium. These structures consist of solitary excitations that manifest themselves as electrical pulses in nerves [1], concentration spots in chemical reactions [2, 3], oscillons in water waves [4, 5] and in granular matter [6, 7], filaments in gas discharges [8, 9], patches and fairy circles in vegetation [10, 11], or feedback and cavity solitons in nonlinear optics [12–18]. More generally, they are referred to as localised dissipative structures (LDSs) or dissipative solitons [19, 20].

Like other solitons, LDSs can interact and collide with each other, sometimes with particle-like characteristics. But while conventional solitons of conservative integrable systems always emerge unscathed from collisions [21], LDSs can form bound states, merge into one, or even annihilate [20]. These complex interactions arise from the non-integrability of nonlinear dissipative systems, and their study is of particular interest to better understand systems outside thermal equilibrium. Merging and annihilation of solitons have been extensively studied experimentally in non-integrable *conservative* systems, mostly with optical waves [22–27], but also, more recently, with matter waves [28]. In contrast, although several authors have reported complex behaviours of ensembles of LDSs in various settings, experimental observations have been uncontrolled and mostly qualitative (see, e.g. [6, 7, 20]). It is only in gas discharges [29] and in vertically driven fluids [5] that quantitative measurements of the interaction laws have been obtained, with [5] also resolving the merging dynamics. These two latter examples are realisations of, respectively, a reaction-diffusion system and a parametrically driven damped nonlinear Schrödinger equation (NLSE) near the 2:1 resonance.

Here we report on a detailed numerical and experimental study of controlled merging and annihilation dynamics of LDSs in a system described by an AC-driven damped NLSE near the 1:1 resonance. Experiments are performed in a nonlinear optical fibre (Kerr) resonator, in which we can excite LDSs at selected and precise positions, and systematically induce their interactions. The interactions are triggered by manipulating the phase profile of the driver; the outcome controllably depends on the driving frequency and strength. Two LDSs either

© 2016 IOP Publishing Ltd and Deutsche Physikalische Gesellschaft

merge into one, or annihilate each other. In both cases, we temporally resolve the collision dynamics and clearly observe the dissipative nature of the interaction through analysis of the energy balance.

2. Model equations and numerical simulations

To better illustrate our experimental findings, we start our discussion by presenting numerical results. In dimensionless form, the AC-driven damped NLSE reads

$$\mathrm{i}\Psi_t + |\Psi|^2\Psi + \Psi_{xx} = -\mathrm{i}\Psi + \mathrm{i}S\mathrm{e}^{\mathrm{i}\Delta t}. \tag{1}$$

This equation represents in our case the mean-field behaviour of a Kerr resonator [30–32], but is also the small amplitude limit of the AC-driven sine-Gordon equation [33, 34]. It has applications in non-equilibrium systems ranging from plasma physics [35] to Josephson junctions [36], highlighting the general applicability of our study. The equation can be cast into an autonomous form by substituting $\Psi(t, x) = \psi(t, x)\,\mathrm{e}^{\mathrm{i}\Delta t}$

$$\mathrm{i}\psi_t + |\psi|^2\psi + \psi_{xx} = -\mathrm{i}\psi + \Delta\psi + \mathrm{i}S \tag{2}$$

which will be used throughout our work. This form is also referred to as the Lugiato–Lefever equation (LLE) [30].

Depending on the driving strength S and its frequency Δ, equation (2) exhibits a range of solutions, which have been extensively investigated [30–34]. Briefly, the simplest steady-state ($\psi_t = 0$) solutions are homogeneous ($\psi_x = 0$), and they satisfy the well-known cubic steady-state equation $X = Y^3 - 2\Delta Y^2 + (\Delta^2 + 1)\,Y$ with $X = |S|^2$ and $Y = |\psi|^2$. The steady-state curve (Y versus X) is single-valued for $\Delta < \sqrt{3}$, whereas for $\Delta > \sqrt{3}$ it assumes an S-shaped hysteresis cycle with three possible states. The latter range is of more relevance to our experimental configuration [16, 17], and thus the focus of our work. Only the upper and lower states that exist for $\Delta > \sqrt{3}$ are homogeneously stable (bistability): the intermediate, negative slope, branch is unconditionally unstable. The upper branch exhibits however a Turing-pattern instability (also known as modulation instability) with respect to inhomogeneous perturbations, which can lead to the formation of a stationary periodic pattern [30]. The lower branch only exhibits such instability close to the folding point for a very small range of parameters ($Y > 1$ and $\sqrt{3} < \Delta < 2$) but is otherwise stable. LDSs can manifest themselves under conditions of coexistence of a patterned solution and a stable homogeneous solution. They can be understood to coincide with the patterned solution over a finite region in x, and with the homogeneous lower-state solution elsewhere [37].

We are interested in the dynamics that take place when two LDSs collide. Unlike conservative solitons, widely separated LDSs of the AC-driven NLSE (or LLE) are phase-locked to the driver, and thus all of them possess identical traits (for given X and Δ), including frequency (Δ) and velocity. Accordingly, unassisted collisions occur only when two LDSs are sufficiently close to interact attractively [38, 39], yet such interactions are difficult to explore controllably. Inducing collisions by suitably modulating the phase of the driver [40–42] addresses that issue. Specifically, given $S(x) = S_0 \exp[\mathrm{i}\phi(x)]$, an LDS at x_L will move towards the local maximum of $\phi(x)$ with a drift velocity of $\mathrm{d}x_\mathrm{L}/\mathrm{d}t = \phi'(x_\mathrm{L})$ [43, 44]. A collision is thus observed when exciting, for example, two LDSs on opposite sides of a local maximum of $\phi(x)$ [42].

To illustrate such induced collisions, we numerically integrate equation (2) using the split-step Fourier method. We assume a Gaussian driver phase profile $\phi(x) = \phi(0)\exp(-x^2/x_0^2)$. To create LDSs symmetrically distributed about the phase maximum at $x = 0$, we use the initial condition

$$\psi(0, x) = \sqrt{2\Delta}\left[\,\mathrm{sech}[\sqrt{\Delta}\,(x - x_\mathrm{L})] + \mathrm{sech}[\sqrt{\Delta}\,(x + x_\mathrm{L})]\right]. \tag{3}$$

The initial LDS separation $2x_\mathrm{L} = 70$ is chosen to be much larger than their characteristic width ($\sim 1/\Delta$) [32–34, 45] so as to avoid any interactions during the transients leading to the LDS formation. Figures 1(a) and (b) show typical results for two different sets of driver frequency Δ and strength S_0, as listed in the caption, and with $\phi(0) = 0.5$ rad and $x_0 = 30$. These parameters are chosen to replicate our experiments. Note that the homogeneous background on which the LDSs are superimposed is only just visible in figures 1(a) and (b) because of its small level, $Y \sim 0.5$. For clarity, the figures neglect the initial portion of the simulation (which lasts for more than $t = 1700$), during which the two LDSs slowly approach each other from their initial separation of $2x_\mathrm{L} = 70$. In both cases, it can be seen that the LDSs drift towards each other until they are close enough to interact. The outcome of the collision is, however, markedly different. Indeed, for $[\Delta, S_0] = [2.91, 1.87]$ the two LDS merge into one (figure 1(a)), while for $[\Delta, S_0] = [3.64, 2.10]$ the intracavity field after the interaction is globally reduced to the homogeneous solution, i.e. the two LDSs annihilate one another (figure 1(b)).

It is apparent that the interactions depend on the parameters of the driver. This has been numerically explored further by systematically varying our four control parameters, Δ, S_0, $\phi(0)$, and x_0, over a wide range. We have found that Δ and S_0 mainly govern the outcome of the collision, while the phase modulation parameters $\phi(0)$ and x_0 mostly determine the speed at which the LDSs approach each other, i.e. set the timing of

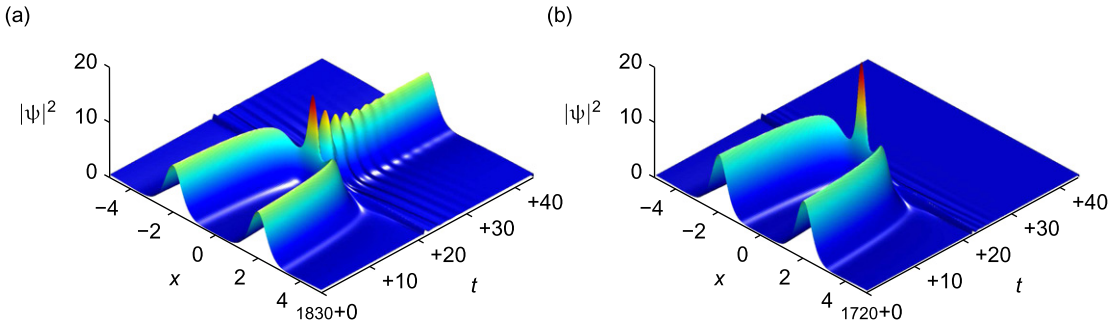

Figure 1. Numerically simulated dynamics of induced LDS interactions for $\phi(0) = 0.5$ rad and $x_0 = 30$. In (a) $[\Delta, S_0] = [2.91, 1.87]$ and two LDSs merge into one; in (b) $[\Delta, S_0] = [3.64, 2.10]$ and two LDSs annihilate one another.

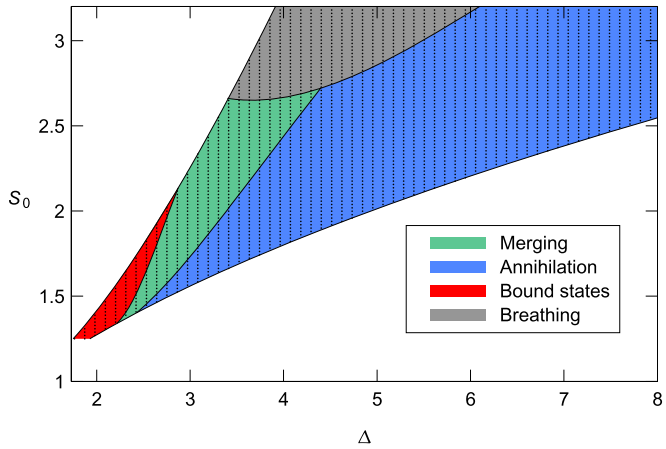

Figure 2. Results from numerical simulations illustrating the outcome of LDS interactions as a function of driving frequency Δ and strength S_0 for $\phi(0) = 0.5$ rad, and $x_0 = 30$. Each solid dot represents a distinct simulation. No LDSs exist in the white-colour coded area.

the collision. In figure 2, we summarise the numerically observed outcome of the interaction as a function of S_0 and Δ for the same driver phase modulation $\phi(x)$ as above. As can be seen, merging (green) and annihilation (blue) occur in clearly distinct, but adjacent, regions. For a given driving strength S_0, the system favours annihilation over merging at higher driving frequencies. This can be related to the closer proximity to the folding point at $\Delta_c \sim \pi^2|S_0|^2/8$, beyond which LDSs cease to exist in this system [33]. Interestingly, in the area marked 'bound states' no collision occurs. Instead, the two LDSs form a stable bound state [38, 46–49]: repulsive interactions of the LDSs resist the drift induced by the driver phase modulation. Not surprisingly, this region slightly grows at the expense of the 'merging' region when a shallower phase modulation is used (the merging/annihilation boundary is mostly unaffected). In the grey region, labelled 'breathing', the individual LDSs exhibit breathing as a result of an underlying Hopf bifurcation [34]. Their interaction can lead either to merging or annihilation, depending on the phase of their breathing at the onset of the collision. The bound-state and breather regimes will not be further discussed here because experimental limitations currently prevent us from observing them. We also note that there exists other systems with overall similar phenomenology, such as those described by Ginzburg–Landau equations, including e.g. fibre lasers [46, 50].

Experimental realisation

We now describe our experimental configuration, implemented in the optical domain. Specifically, we induce controllable LDS interactions in a coherently driven passive optical fibre resonator that exhibits instantaneous Kerr nonlinearity. In the high-finesse limit, this system is known to be governed by the LLE (2), with $\psi(t, x)$ representing the slowly varying envelope of the electric field [31]. The LDSs of such Kerr resonator have been observed experimentally before and are usually referred to as temporal cavity solitons [16–18]. These are pulses of light that continuously circulate in the resonator, yet remain stationary in a reference frame that is moving at

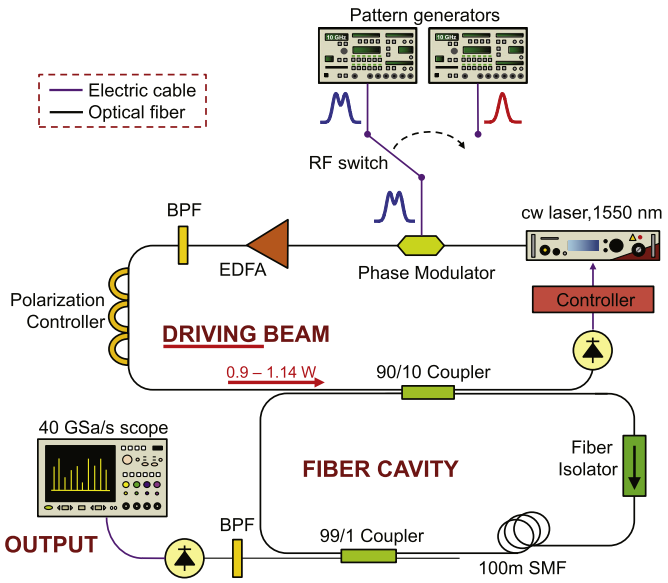

Figure 3. Experimental setup. cw: continuous-wave, EDFA: erbium-doped fibre amplifier, BPF: band-pass-filter, SMF: single-mode fibre.

the group velocity of the driving light in the fibre. The transverse coordinate x in equation (2) is thus a 'fast-time' $x \rightarrow \tau$ that is defined in such a reference frame and that allows to describe the temporal profile of the field envelope. In contrast, t is a 'slow-time' that describes changes in the field envelope over consecutive roundtrips around the resonator. The normalisation is such that dimensional time-scales τ' and t' (units of s) and the electric field envelope $E(t', \tau')$ (units of $\mathrm{W}^{1/2}$) are related to the dimensionless variables in equation (2) by [16]

$$t = \alpha \frac{t'}{t_{\mathrm{R}}}, \qquad \tau = \tau' \sqrt{\frac{2\alpha}{|\beta_2| L}}, \qquad \psi = E \sqrt{\frac{\gamma L}{\alpha}}. \tag{4}$$

Here t_{R} is the roundtrip-time of the resonator, α is equal to half the percentage of total power loss per round-trip, L is the resonator length, and $\beta_2\,(<0)$ and γ are, respectively, the anomalous group-velocity dispersion and Kerr nonlinearity coefficients of the fibre. The driving strength S_0 is related to the power P_{in} of the continuous-wave (cw) laser driving the resonator as $S_0 = (P_{\mathrm{in}}\gamma L\theta/\alpha^3)^{1/2}$, where θ is the intensity transmission coefficient of the coupler used to inject the field into the resonator. Finally, Δ characterises the frequency detuning of the cw driving laser at ω from the closest resonator resonance at ω_0, $\Delta \simeq t_{\mathrm{R}}(\omega_0 - \omega)/\alpha$.

A detailed schematic of our experimental setup is shown in figure 3. Overall, it is similar to the ones used in [44, 51]. Note that these two previous studies were concerned with the manipulation of widely separated solitons, that were fully independent from one another; here in contrast we use similar tools to induce and study *collisions* of LDSs, i.e. a configuration in which solitons are closely interacting. As a coherent driver, we use a narrow linewidth cw laser at 1550 nm wavelength, which is amplified up to 1.14 W using an erbium-doped fibre amplifier (EDFA) before being coupled into the resonator by a 90/10 fibre coupler ($\theta = 0.1$). Noise accumulated during the amplification stage is mostly removed with an optical band-pass filter (BPF). The resonator is composed of 100 m of standard silica single-mode fibre (SMF), with $\beta_2 = -21.4\ \mathrm{ps}^2\,\mathrm{km}^{-1}$ and $\gamma = 1.2\ \mathrm{W}^{-1}\,\mathrm{km}^{-1}$. It also incorporates an optical isolator to prevent resonance of stimulated Brillouin scattering radiation, and a 99/1 fibre coupler through which the intracavity dynamics are monitored with a fast photodiode and a real-time oscilloscope. The overall finesse of the resonator was measured to be $\mathcal{F} = \pi/\alpha \sim 21.5$. The BPF at the 1% output filters out the homogeneous cw background that coexists with the LDSs, thereby improving the signal-to-noise ratio of our data [16]. The resonance frequencies of our optical fibre ring generally exhibit fluctuations due to environmental perturbations. To maintain a fixed Δ, we therefore actively actuate the driving laser frequency to follow any changes in the resonances, by locking to a set level the optical power reflected off the resonator input [16, 17, 44]. Changing the lock point allows us to controllably adjust Δ, but we remark that the accuracy with which we can do so is insufficient to explore the formation of bound states since they manifest themselves over a narrow range of driver frequencies (see figure 2). In this context, we also note that, with our current configuration, we are unable to reach power levels required to explore interactions of breathing LDSs.

To controllably induce LDS interactions, we phase modulate the resonator driving field with a 10 GHz electro–optic modulator. The modulator is driven by one of two 10 GHz programmable pattern generators,

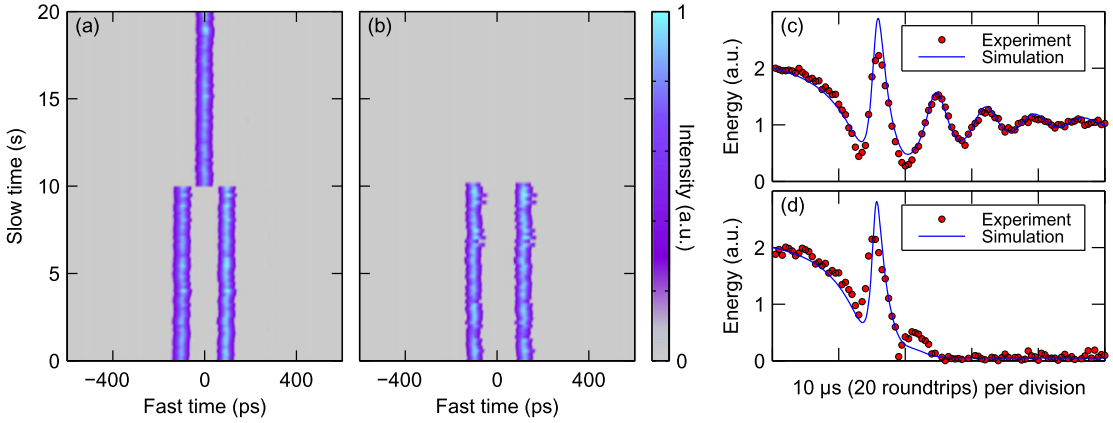

Figure 4. (a), (b) Experimental density plots showing the evolution of the intracavity temporal intensity profile as two LDSs (a) merge into one, and (b) annihilate each other. The successive traces are recorded with a real-time oscilloscope at 1 frame s^{-1}. (c), (d) The roundtrip-to-roundtrip evolution of the total intracavity energy during LDS (c) merging and (d) annihilation. The experimental data is represented by red circles, and results from numerical simulations are shown as blue solid lines.

selected with an electronic switch. The pattern generators are synchronised to each other by a single external clock, such that the repetition rate of their output patterns is identical to the resonator free-spectral range. The first generator (left in figure 3) is configured to produce a pattern of two 130 ps full-width-at-half-maximum electronic pulses with 200 ps separation. These are fed to the phase modulator in the initial stage of the experiment. During that stage, we mechanically perturb the resonator, which results in the direct excitation of two LDSs at the two phase maxima [51]. After the LDSs are stably formed and trapped at the maxima [44], we activate the electronic switch and the phase modulator feed is abruptly changed (within a few nanoseconds) to the output of the second pattern generator. That generator is set to produce a pattern made up of a single pulse whose delay is adjusted to lie halfway between the two pulses generated by the first generator. Accordingly, the LDSs in the resonator find themselves approximately symmetrically positioned about the new single maximum of the phase profile. As in the simulations of figure 1, the LDSs thus start drifting towards that maximum, interacting once sufficiently close to each other. Note that the new driver phase profile takes a few photon lifetimes ($\sim$1 μs) to get imprinted inside the resonator after the switch, but that transient is negligible compared to the time it takes for the LDSs to collide/interact. Also, we have carefully verified that the $\sim$0.5 rad phase modulation amplitude used in our experiments is small enough for the abrupt switch in phase profile not to directly excite or erase LDSs as in [51].

The temporal intensity profile of the intracavity light measured at the 1% output of the resonator is recorded every second by the oscilloscope (triggered by the pattern generators). Typical results are shown in figures 4(a) and (b) as density plots representing vertical concatenations of successive recordings that have been obtained for $[\Delta, S_0] = [2.91, 1.87]$ and $[3.64, 2.10]$, respectively. The first 10 s of the measurements are very similar: two LDSs with 200 ps separation are stably trapped at the maxima of the phase pulses defined by the first pattern generator. After switching to the single phase pulse pattern (which occurs at $t \simeq 10$ s) and inducing the LDS interaction, a single LDS is seen to remain for $[\Delta, S_0] = [2.91, 1.87]$ while both disappear when $[\Delta, S_0] = [3.64, 2.10]$. These results are strongly indicative of merging and annihilation, which is in agreement with numerical simulations. Indeed, the simulation results in figure 1 use the very same parameters as the experiments here. Yet, these results are limited by the slow 1 frame per second acquisition rate of the oscilloscope, which hinders direct interpretation.

To clearly establish the origin of the observed dynamics, we have recorded the roundtrip-by-roundtrip evolution of the intracavity energy on the real-time oscilloscope. Typical experimental results for merging and annihilation are shown as red circles in figures 4(c) and (d), respectively. Here we have normalised the energy such that a single isolated LDS carries an energy of 1 in arbitrary units. The results unambiguously reveal the dissipative nature of the interactions: for $[\Delta, S_0] = [2.91, 1.87]$ the energy falls from two to one, implying merging; for $[\Delta, S_0] = [3.64, 2.10]$ the energy falls from two to zero, implying annihilation. Note that for the sake of clarity we only show short 50 μs long segments of the overall evolutions during which the interaction dynamics take place. These segments were recorded approximately 5 ms after the electronic switch controlling the phase modulation feed was activated. We note that this large delay further highlights that our results cannot be explained in terms of direct LDS erasure (and excitation) by the abrupt switch in phase profile. Indeed, such dynamics typically occur in less than 100 μs, i.e. two orders of magnitude faster [51]. In fact, the 5 ms delay agrees well with the time expected for the LDSs to drift sufficiently close to each other to interact, as confirmed by

full numerical simulations of our experiment with equation (2) and that predict a 6.1 ms (5.8 ms) delay for merging (annihilation), respectively. (Small discrepancies can be attributed to experimental uncertainties.) As a final confirmation, in figures 4(c) and (d) we also plot, as blue solid lines, the energy evolutions extracted from the numerically simulated merging and annihilation events shown in figure 1 (post-processed to take into account the BPF at the resonator output). The outstanding agreement clearly confirms that merging and annihilation of LDSs occur in our experiment.

3. Conclusions

We have demonstrated, to the best of our knowledge, the first example of experimentally controlled interactions of LDSs. Our study also provides the first quantitative analysis of such interactions in an AC-driven nonlinear Schrödinger system, and more generally, in any nonlinear dissipative system near the 1:1 resonance. We have numerically identified a diversity of interaction scenarios for different parameters of the system driver. Experiments performed in an optical resonator show unequivocal evidence of possible selection of LDS interaction by the operator from merging to annihilation and paves the way to similar controlled experiments in other systems [52]. These soliton interactions are fundamentally different from their counterparts in conservative integrable systems where localised structures typically tunnel through each other. Controllable outcome of the interaction process could potentially find application in the coding of optical signals in optical information processing and communications.

Acknowledgments

We acknowledge financial support from the Marsden fund of the Royal Society of New Zealand. M Erkintalo also acknowledges support from the Finnish Cultural Foundation.

References

[1] Hodgkin A L and Huxley A F 1952 *J. Physiol.* **117** 500–44
[2] Pearson J E 1993 *Science* **261** 189–92
[3] Lee K J, McCormick W D, Ouyang Q and Swinney H L 1993 *Science* **261** 192–4
[4] Wu J, Keolian R and Rudnick I 1984 *Phys. Rev. Lett.* **52** 1421–4
[5] Clerc M G, Coulibaly S, Mujica N, Navarro R and Sauma T 2009 *Phil. Trans. R. Soc.* A **367** 3213–26
[6] Umbanhowar P B, Melo F and Swinney H L 1996 *Nature* **382** 793–6
[7] Lioubashevski O, Arbell H and Fineberg J 1996 *Phys. Rev. Lett.* **76** 3959–62
[8] Astrov Yu A and Logvin Yu A 1997 *Phys. Rev. Lett.* **79** 2983–6
[9] Astrov Yu A and Purwins H-G 2001 *Phys. Lett.* A **283** 349–54
[10] Lejeune O, Tlidi M and Couteron P 2002 *Phys. Rev.* E **66** 010901
[11] Fernandez-Oto C, Tlidi M, Escaff D and Clerc M G 2014 *Phil. Trans. R. Soc.* A **372** 20140009
[12] Taranenko V B, Staliunas K and Weiss C O 1997 *Phys. Rev.* A **56** 1582–91
[13] Schäpers B, Feldmann M, Ackemann T and Lange W 2000 *Phys. Rev. Lett.* **85** 748–51
[14] Barland S *et al* 2002 *Nature* **419** 699–702
[15] Ackemann T, Firth W J and Oppo G-L 2009 *Adv. At. Mol. Opt. Phys.* **57** 323–421
[16] Leo F, Coen S, Kockaert P, Gorza S-P, Emplit Ph and Haelterman M 2010 *Nat. Photon.* **4** 471–6
[17] Jang J K, Erkintalo M, Murdoch S G and Coen S 2013 *Nat. Photon.* **7** 657–63
[18] Herr T, Brasch V, Jost J D, Wang C Y, Kondratiev N M, Gorodetsky M L and Kippenberg T J 2014 *Nat. Photon.* **8** 145–52
[19] Akhmediev N N and Ankiewicz A ed 2008 *Dissipative Solitons: From Optics to Biology and Medicine* (Berlin: Springer)
[20] Purwins H-G, Bödeker H U and Amiranashvili Sh 2010 *Adv. Phys.* **59** 485–701
[21] Zakharov V E and Shabat A B 1973 *Sov. Phys. JETP* **37** 823–8
[22] Shih M-f, Segev M and Salamo G 1997 *Phys. Rev. Lett.* **78** 2551–4
[23] Rotschild C, Alfassi B, Cohen O and Segev M 2006 *Nat. Phys.* **2** 769–74
[24] Tikhonenko V, Christou J and Luther-Davies B 1996 *Phys. Rev. Lett.* **76** 2698–701
[25] Shih M-f and Segev M 1996 *Opt. Lett.* **21** 1538–40
[26] Królikowski W and Holmstrom S A 1997 *Opt. Lett.* **22** 369–71
[27] Królikowski W, Luther-Davies B, Denz C and Tschudi T 1998 *Opt. Lett.* **23** 97–9
[28] Nguyen J H V, Dyke P, Luo D, Malomed B A and Hulet R G 2014 *Nat. Phys.* **10** 918–22
[29] Bödeker H U, Liehr A W, Frank T D, Friedrich R and Purwins H-G 2004 *New J. Phys.* **6** 62
[30] Lugiato L A and Lefever R 1987 *Phys. Rev. Lett.* **58** 2209–11
[31] Haelterman M, Trillo S and Wabnitz S 1992 *Opt. Commun.* **91** 401–7
[32] Wabnitz S 1993 *Opt. Lett.* **18** 601–3
[33] Barashenkov I V and Smirnov Yu S 1996 *Phys. Rev.* E **54** 5707–25
[34] Barashenkov I V and Zemlyanaya E V 1999 *Physica* D **132** 363–72
[35] Kim H C, Stenzel R L and Wong A Y 1974 *Phys. Rev. Lett.* **33** 886–9
[36] Ustinov A V 1998 *Physica* D **123** 315–29
[37] Lugiato L A 2003 *IEEE J. Quantum Electron.* **39** 193–6
[38] Cai D, Bishop A R, Grønbech-Jensen N and Malomed B A 1994 *Phys. Rev.* E **49** 1677–9

[39] Brambilla M, Lugiato L A and Stefani M 1996 *Europhys. Lett.* **34** 109–14
[40] Rozanov N N 1992 *Opt. Spectrosc.* **72** 243–6
[41] Rosanov N N, Fedorov A V, Fedorov S V and Khodova G V 1993 Diffractive transverse patterns in wide-aperture passive and active nonlinear optical systems and discrete-analogous method for nonlinear optical processing of information SPIE **2039** pp 330–41
[42] McIntyre C, Yao A M, Oppo G-L, Prati F and Tissoni G 2010 *Phys. Rev.* A **81** 013838
[43] Firth W J and Scroggie A J 1996 *Phys. Rev. Lett.* **76** 1623–6
[44] Jang J K, Erkintalo M, Coen S and Murdoch S G 2015 *Nat. Commun.* **6** 7370
[45] Coen S and Erkintalo M 2013 *Opt. Lett.* **38** 1790–2
[46] Afanasjev V V, Malomed B A and Chu P L 1997 *Phys. Rev.* E **56** 6020–5
[47] Barashenkov I V, Smirnov Yu S and Alexeeva N V 1998 *Phys. Rev.* E **57** 2350–64
[48] Grelu P and Akhmediev N 2004 *Opt. Express* **12** 3184–9
[49] Rosanov N N, Fedorov S V and Shatsev A N 2009 *Opt. Spectrosc.* **106** 869–74
[50] Grelu P and Akhmediev N 2012 *Nat. Photon.* **6** 84–92
[51] Jang J K, Erkintalo M, Murdoch S G and Coen S 2015 *Opt. Lett.* **40** 4755–8
[52] Besse V, Leblond H, Mihalache D and Malomed B A 2014 *Opt. Commun.* **332** 279–91